Energy Conversion and Management 124 (2016) 287–296

Contents lists available at ScienceDirect

Energy Conversion and Management

journal homepage: www.elsevier.com/locate/enconman

A hybrid desalination system using humidification-dehumidification and solar stills integrated with evacuated solar water heater

S.W. Sharshir [a,b,c], Guilong Peng [a,b], Nuo Yang [a,b,*], Mohamed A. Eltawil [d], Mohamed Kamal Ahmed Ali [e], A.E. Kabeel [f]

[a] Nano Interface Center for Energy (NICE), School of Energy and Power Engineering, Huazhong University of Science and Technology, Wuhan 430074, China
[b] State Key Laboratory of Coal Combustion, Huazhong University of Science and Technology, Wuhan 430074, China
[c] Mechanical Engineering Department, Faculty of Engineering, Kafrelsheikh University, Kafrelsheikh, Egypt
[d] Agricultural Engineering Department, Faculty of Agriculture, 33516, Kafrelsheikh University, Egypt
[e] Automotive and Tractors Engineering Department, Faculty of Engineering, Kafrelsheikh University, Kafrelsheikh, Egypt
[f] Mechanical Power Engineering Department, Faculty of Engineering, Tanta University, Tanta, Egypt

ARTICLE INFO

Article history:
Received 9 April 2016
Received in revised form 9 July 2016
Accepted 11 July 2016

Keywords:
Hybrid system
Solar stills
Humidification-dehumidification
Solar desalination
Gain-Output-Ratio

ABSTRACT

This paper offers a hybrid solar desalination system comprising a humidification-dehumidification and four solar stills. The developed hybrid desalination system reuses the drain warm water from humidification-dehumidification to feed solar stills to stop the massive warm water loss during desalination. Reusing the drain warm water increases the gain output ratio of the system by 50% and also increased the efficiency of single solar still to about 90%. Furthermore, the production of a single solar still as a part of the hybrid system was more than that of the conventional one by approximately 200%. The daily water production of the conventional one, single solar still, four solar still, humidification- dehumidification and hybrid system were 3.2, 10.5, 42, 24.3 and 66.3 kg/day, respectively. Furthermore, the cost per unit liter of distillate from conventional one, humidification- dehumidification and hybrid system were around \$0.049, \$0.058 and \$0.034, respectively.

1. Introduction

Freshwater water shortage is considered one of the most serious challenges to human beings [1]. Freshwater is extremely important to sustain human life. The demand for freshwater is increasing rapidly by increasing the population growth. Lakes, rivers, and underground water are the main water sources. The problem may result from the fact that most of them are polluted. Furthermore, some of them have level of salt concentration more than the suitable range of 500 ppm [2]. The excessive use of fertilizers and chemical insecticides/pesticide in agriculture purposes is also an important issue for water pollution [3].

The polluted water is not only destructive for the human health but also for all organisms in this world. For example, the water-borne diseases spread through polluted water. The freshwater demand for many public places like hospitals, chemical industries, battery maintenance and laboratories, largely exceed the amount that freshwater sources can meet. Desalination is very important technologies to solve the water scarcity by using solar energy. Where conventional techniques for desalination need considerable amount of energy and pollute the environment due to the resulting gases [4].

Due to the simplicity and no need of conventional energy, the humidification- dehumidification (HDH) received a great concern during the past few years [5,6]. The principle of solar HDH desalination cycles depends on enhancing system efficiency by recovering the energy of condensation and evaporation. Mohamed and El-Minshawy [7] investigated the performance of HDH desalination unit theoretically under different parameters.

The effect of the various system configurations, operating and meteorological parameters on the output of a HDH system was studied theoretically and experimentally [8–10]. The preheating gave a high yield of about 22 L/day at a price of \$0.0578/l [10]. Ghazal et al. [11] examined experimentally a small HDH unit to enhance its performance. The air and water heaters as well as traditional evaporator of HDH unit were changed with compact unit designs. Two different types of cellulosic (Honeycomb) evaporative cooling pads assembled of corrugated papers were experimentally investigated by Malli et al. [12]. Nafey et al. [13] developed a model to calculate the output of a small desalination unit using flashing procedure under various operating conditions.

* Corresponding author.
E-mail address: nuo@hust.edu.cn (N. Yang).

http://dx.doi.org/10.1016/j.enconman.2016.07.028
0196-8904/

Nomenclature

CSS	conventional solar still
SSS	single solar still
FSS	four solar still
HDH	humidification-dehumidification
HSDS	hybrid solar desalination system
A	area of solar still, m^2
Cp	heat capacity, J/kg °C
d	distance between water and glazier
h_{bw}	convection heat transfer coefficient between the basin and non-potable water, W/m^2 °C
h_{ca}	convection heat transfer coefficient with the ambient, W/m^2 °C
h_{cw}	convection heat transfer coefficient between the water in basin and glazier, W/m^2 °C
h_{fgss}	latent heat of vaporization for solar still, J/kg
I(t)	solar insolation normal to glazier cover, W/m^2
m	mass, kg
m_{dss}	rate of mass evaporation, kg/s
m_{dHDH}	rate of distillate from HDH, kg/day
p_g	water vapor pressure at glazier temperature, Pa
p_w	water vapor pressure at water temperature, Pa
Q_{bw}	heat transfer from basin to water in basin, W
Q_{cg}	heat transfer from glazier to ambient, W
Q_{cw}	heat transfer from water in basin to glazier, W
Q_e	heat transfer due to evaporation, W
Q_{loss}	heat transfer from basin to ambient, W
Q_{mw}	energy needed to heat makeup water to water basin temperature, W
Q_{rg}	radiation heat transfer from glazier to ambient, W
Q_{rw}	radiation heat transfer from water in basin to glazier, W
T	temperature, °C
V_a	wind velocity, m/s
K_w	non-potable water thermal conductivity, W/m K
K	conduction heat transfer
U	heat loss coefficient from basin and sides to ambient, W/m^2 K
Pr	Prandtle number
Gr′	Grashof number
L	rectangle length

Greek letters

α	absorption coefficient
ε	emissivity coefficient
σ	Stefan-Boltzmann constant, W/m^2 K^4

Subscripts

a	ambient
b	basin
g	glass
sky	sky
w	water in basin

Yıldırım and Solmus [14] investigated the performance of HDH desalination unit theoretically at different unit design and operating conditions. They pointed out that water heating has a critical impact on the yield of freshwater. Hou et al. [15] studied theoretically the hybrid of the multi HDH and the basin type. The gain output ratio (GOR) of the studied system was improved by 2–3 times during reusing the drained.

Besides HDH, solar still (SS) is another popular method of desalination. SS is considered an alternative source of potable or fresh water, but owing to its low output, it is not applied widely. Several researchers have redesigned or developed structures which were investigated experimentally and theoretically to enhance the output of the SS such as the insulation thickness [16], indirect evaporator–condenser [17], change of water depth [18], sponge cubes [19], stepped SS with reflectors [20], phase change materials (PCMs) [21], wind speed [22], and the effect of climatological, operational and design variables [23].

Furthermore, the rate of mass transfer basically relies on the temperature variation between the glazier and basin water [24,25]. It's well known that preheating of water that feed to SS is carried out to increase the water- glass temperature difference and consequently enhance the still yield. It is easy to preheat the feed water by integrating the SS with a collector [26] and incorporating a water heater into the desalination still [27]. However, using solar collectors increases the expenditure of the desalination system and reduces the overall efficiency of SS.

Velmurugan et al. [28] has incorporated fins at the basin of the SS and reported that the freshwater improved by about 45.5%. El-Agouz et al. [29] studied the performance of a steeped SS with and without a water closed loop. They showed that steeped SS with a make-up water reinforce the freshwater output by 57.2% compared to traditional still.

Samuel et al. [30] used various types of priceless energy storage material to improve the CSS productivity. The performance of CSS was evaluated theoretically and experimentally. The results illustrated that the output of freshwater using ball-shape as a heat storage and sponge reaches the extreme yield of 68.18% and 22.72%, respectively compared with CSS. Kabeel et al. [31] examined experimentally the influence of using a double passes air collector with PCMs on the SS productivity. The results illustrated that, the freshwater yield was increased by 108%.

Omara et al. [32] have conducted an experimental modification to examine the performance of a hybrid solar desalination system (HSDS) which consists of corrugated and wick absorbers of SSs combined with external condenser. Results indicated that the corrugated wick SS with reflector produced fresh water about 180% greater than that of CSS in the presence of vacuum.

In this study, the rejected warm water from HDH is used to feed FSS instead of using solar collectors, so that the thermal performance increases and the cost will be decreased**.** According to the energy analysis, utilization of HSDS aims to enhance the freshwater output and minimize the cost per liter. The rejected warm water from HDH unit is reused to improve the SSs productivity throughout the day.

The contributions of this work are:

1. Comparing the fresh water yield of the HSDS with HDH and CSS separately.
2. Comparing the performance of the HSDS with HDH and CSS separately.
3. Economic evaluation of HSDS productivity (cost/liter) compared with HDH and CSS separately.
4. Investigating the influence of insulation thickness on both the yield and efficiency.

2. System description

The system comprises of two units. The first unit was a solar HDH as described in Hamed et al. [10]. The rejected warm water from HDH was enough to feed total area of 4 m^2. So, four-solar

stills (FSS) with 1 m^2 base surface area for each still were used. According to theoretical calculation, if the base surface area increases above 1 m^2, the losses will be increased while, the productivity will be decreased. Meanwhile, decreasing the surface area below 1 m^2 will increase the productivity slightly. Moreover, using of FSS with 1 m^2 base surface area for each still is the preferred design because it is better and easier than large one in the manufacturing, maintenance, transportation and insulation. Also, the thickness of the glass is very small about 4 mm and easily to be broken with large area of basin hence, four stills with small area are better than one still with large area.

A detailed drawing of a HSDS is shown in Fig. 1. The solar HDH unit consisted of two vertical ducts joined together from the upper and the lower, forming a closed loop for air circulation and an open loop for water circulation. More details about HDH can be found in [10,33]. The condensate water was aggregated from the nethermost of the dehumidifier (condenser). The rejected warm water from the nethermost of humidifier (evaporator) was pumped to an isolated tank to be desalinated in a FSS unit to produce fresh water further. The FSS unit can work continuously during day time and night time. The description of the hybrid system is presented in Table 1.

2.1. Experimental procedures for humidification-dehumidification

The experiments carried out during the period from 1st of June to end of August 2014 at the Faculty of Engineering, Kafrelsheikh University, Egypt, (Latitude 31.07°N and longitude 30.57°E). From the obtained results in Ref. [10], the maximum amelioration in the yield was obtained when HDH system was operated in the afternoon from 13:00 pm to 17:00 pm. Solar collector operated on the requisite principle of using the solar radiation to heat the water. Hot water tubes were powered by solar energy, then the hot water went up through insulated tubes to storage tank by natural convection. The experimental results clarified that maximum solar intensity was about 1100 W/m^2 at noon as shown in Fig 2. Stored energy inside the collector from the morning to 13:00 pm caused an increase in the water temperature in the collector up to 84–87 °C. The operation involves two steps. In the first (experimental) step, HDH system operated from 13:00 pm to 18:00 pm and the rejected warm water from the humidifier nethermost with high temperature of about 60–75 °C moved to an insulated storage tank. In the second (theoretical) step, the stored water in the isolated tank fed the FSS at high temperature during night-time.

2.2. Error analysis for humidification-dehumidification unit

Through the experiments, some parameters were gauged for performance evaluation of the desalination system. The required quantities to be gauged are water flow rate and air streams, water temperature at entrance and exodus of the storage tank, temperatures of water and air at the entrance and exodus of humidifier, dehumidifier, RH of air at entrance and exodus of humidifier, dehumidifier and the yield of the unit. Table 2 illustrates the accuracy, range and uncertainty errors of each measuring instrument.

2.3. Theoretical modeling for solar stills

Equations of energy balance for the SSs are presented for three regions: Non-potable water (saline water), absorber plate (basin) and glazier. The temperatures of non-potable water, basin plate and glazier cover is estimated at every moment. By the use of MATLAB program, the differential equation is solved. The next suppositions are taken into consideration for the SSs energy equations:

- Steady state condition through the SSs
- The glazier is suggested to be thin sufficient to hinder assimilation of any incident radiation and the glazier conduction resistance could be abandoned.
- The SSs prohibit infiltration of vapor.

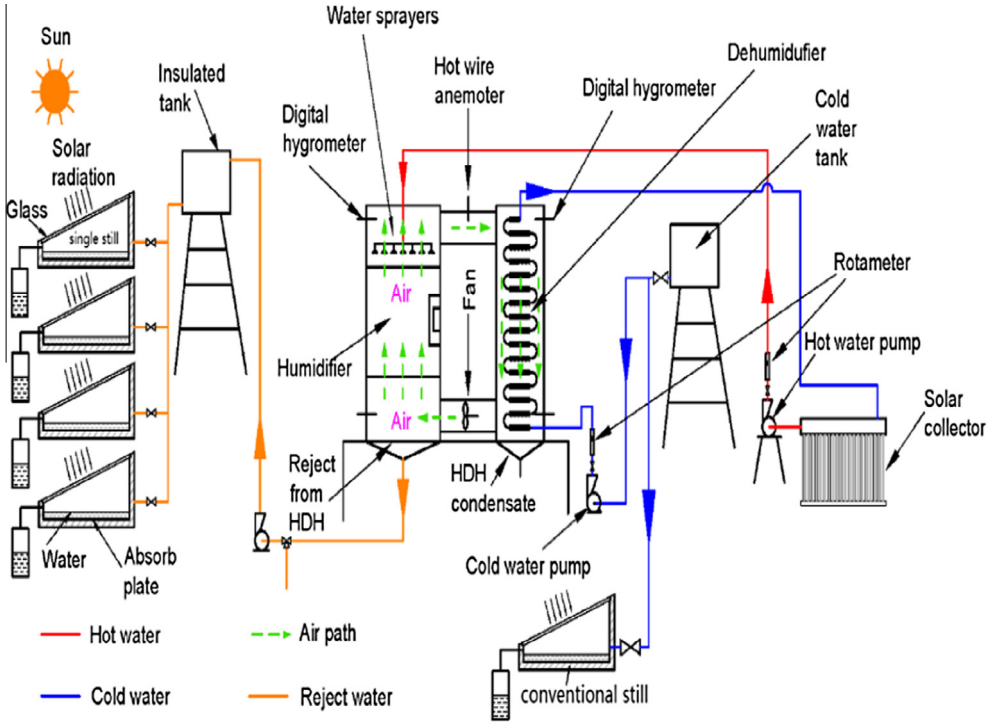

Fig. 1. Detailed drawing of the experimental setup.

Table 1
Technical specifications of hybrid system components.

Technical specification	Value
Humidifier	
Thickness of galvanized sheet, mm	1.5
Dimensions (length × width × height), cm	80 × 50 × 200
Packing material cellulose type with overall surface area, m^2	10
Dehumidifier	
Thickness of galvanized sheet, mm	1.5
Shape	Cylindrical
Diameter, cm	40
Height, cm	200
Length of copper coil, m	15
Thickness of coil, mm	1.5
Outer diameter, cm	1.27
Attached by copper corrugated fins	
Vacuum collector	
Projected area	2
Vacuum tubes	
Shape	20
Cylindrical	
Material type	Stainless steel
Insulation material	Polyurethane foam
Insulation thickness, cm	5
Capacity, l	220
Fans and pumps	
Pump type	Centrifugal
Number of pumps	3
Pumps power, W	373
Electric propeller power, W	15
Water tanks	
Cold water tank, l	250
Type of material	PVC
Thickness, mm	2
Capacity of the insulated tank, liters	300
Material of insulated tank	Steel
Thickness of insulated tank, mm	1.5
Solar still (for each still)	
Basin area, m^2	1
Basin dimension, cm	100 × 100
Glass area, m^2	1
Depth of water in still, cm	1
Depth of high-side wall, cm	45
Depth of low side wall, cm	16
Glazier cover with thickness, mm	4

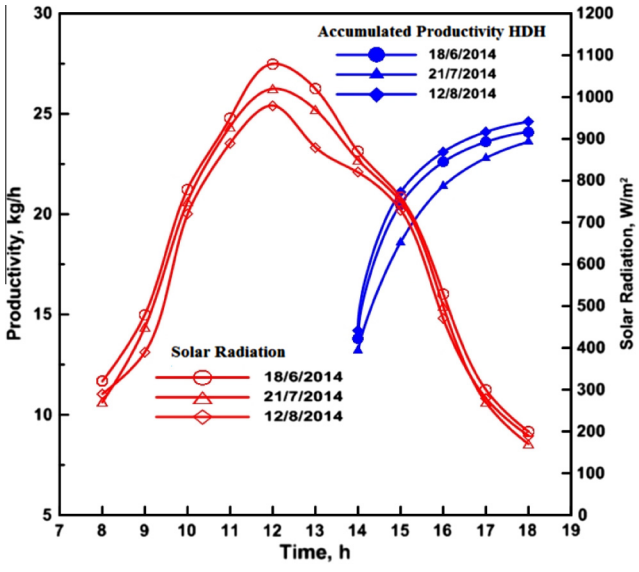

Fig. 2. Cumulative productivity and solar radiation with time.

Table 2
Experimental measurements, accuracy, range, uncertainty errors.

Instrument	Accuracy	Range	% Error
Solar meter, to measure solar intensity	±1.00 W/m^2	0–2000 W/m^2	1.5
Temperature indicator, thermocouples of K-type	±0.10 °C	0–100 °C	1.5
Humidity sensor, to measure the relative humidity	±1.50% RH	0–100% RH	1
Air meter, to measure air speed	±0.1 m/s	0.0–10 m/s	0.75
Water meter, to measure both of cold and hot water flow rate, L/min	±0.1 L/min	0.02–8 L/min	1

Energy balance for the basin (absorber plate) [34]

$$m_b c_{pb}(dT_b/dt) = I(t)A_b\alpha_b - Q_{bw} - Q_{loss} \quad (1)$$

Energy balance for the non-potable water [35,36]

$$m_w c_{pw}(dT_w/dt) = I(t)A_w\alpha_w + Q_{bw} - Q_{cw} - Q_{rw} - Q_e - Q_{mw} \quad (2)$$

Energy balance for the glazier [34],

$$m_g c_{pg}(dT_g/dt) = I(t)A_g\alpha_g + Q_{cw} + Q_{rw} + Q_e - Q_{rg} - Q_{cg} \quad (3)$$

The rate of the convection heat transfer between the basin and the water [36,37],

$$Q_{bw} = h_{bw}A_b(T_b - T_w) \quad (4)$$

The coefficient of heat transfer by convection between the basin and the non-potable water, h_{bw} is given as 135 W/m^2 K [36,37]

Or according to Ref. [38] h_{bw} is equal:

$$h_{bw} = 0.54\frac{K_w}{L}(GrPr)^{0.25} \quad (5)$$

The above equation variables are defined in Appendix A and Nomenclature.

The rate of the heat losses by convection over the basin bottom and sides is expressed as [39],

$$Q_{loss} = U_b A_b(T_b - T_a) \quad (6)$$

where $U_b = K_i/L_i$, and K_i, L_i are thermal conductivity and insulation thickness, respectively.

The heat transfer rate by convection between non-potable water and glazier is expressed by [36,37].

$$Q_{cw} = h_{cw}A_w(T_w - T_g) \quad (7)$$

whereas the coefficient of heat transfer by convection between the non-potable water and the glazier is expressed by [40],

$$h_{cw} = 0.884\left\{(T_w - T_g) + \frac{(p_w - p_g)\times(T_w + 273)}{(268{,}900 - p_w)}\right\}^{1/3} \quad (8)$$

whereas

$$p_w = e^{\left(25.317 - \frac{5144}{Tw+273}\right)} \quad (9)$$

$$p_g = e^{\left(25.317 - \frac{5144}{Tg+273}\right)} \quad (10)$$

Or according to Ref. [38] h_{cw} equals;

$$h_{cw} = \frac{K}{d}1.22(Gr'Pr)^{0.22} \quad (11)$$

The above equation variables are defined in Appendix A and Nomenclature

The rate of heat transfer by radiation from the basin liner to the glazier is expected from [35],

$$Q_{rw} = \sigma \varepsilon_{eq} A_w \left((T_w + 273)^4 - (T_g + 273)^4 \right) \quad (12)$$

whereas

$$\varepsilon_{eq} = \left[\frac{1}{\varepsilon_w} + \frac{1}{\varepsilon_g} - 1 \right]^{-1} \quad (13)$$

The rate of heat transfer by evaporation between the Non-potable water and the glazier is expressed by [36,37],

$$Q_e = (16.237 \times 10^{-3}) h_{cw} A_w (p_w - p_g) \quad (14)$$

The heat taken by the makeup water is deduced from [35],

$$Q_{mw} = m_{dss} C_w (T_a - T_w) \quad (15)$$

The heat transfer rate by radiation between the glazier cover and sky Q_{rg} is expressed by [16,34],

$$Q_{rg} = \varepsilon_g A_g \sigma \left((T_g + 273)^4 - (T_{sky} + 273)^4 \right) \quad (16)$$

The sky temperature is taken from [40],

$$T_{sky} = T_a - 6.0 \quad (17)$$

or

$$T_{Sky} = 0.0552 \times T_a^{1.5} \quad (18)$$

The heat transfer rate by convection between the glazier and the sky is expressed by [41],

$$Q_{cg} = h_{ca} A_g (T_g - T_{sky}) \quad (19)$$

where h_{ac} is taken from [42],

$$h_{ca} = 5.7 + 3.8 \times V_a \quad (20)$$

Solar still yield

$$m_{dss} = \frac{Q_e}{h_{fg}} \quad (21)$$

The daily efficiency, η_d, is obtained by [41]

$$\eta_d = \frac{\sum m_{dss} \times h_{fg}}{\sum I(t) \times A} \quad (22)$$

where m_{dss} is the accumulation of the hourly yield, h_{fg} is the evaporation latent heat, $I(t)$ is the daily mean solar radiation, A is the full area of the system.

At the first repetition non-potable water, basin and glazier temperatures are substituted by the temperature of air and the basin temperature increase (dT_b), temperature of non-potable water (dT_w) and glazier temperature (dT_g) are calculated by solving Eqs. (1)–(3) of CSS. The 1st order backward difference formula is used to solve the equations numerically. The time interval of each step is 1 s. In the next time step, the parameters are redefined as follows $T_b = T_b + dT_b$, $T_w = T_w + dT_w$ and $T_g = T_g + dT_g$. For real environmental conditions, the intensity I(t) and ambient temperature (T_a) were recorded at several days from 8 am to 18 pm during June to August 2014. Depending upon the environmental conditions, the ambient temperature, speed of air and insolation were varied from 25 to 35 °C; from 0.15 to 3.75 m/s and from 25 to 1100 W/m^2, respectively during different days. The mean values of solar intensity and air temperature were applied. The variables employed in the calculations are given in Table 3. The physical variables involved are taken as similar to that given by Ref. [43].

Table 3
Variables values of mathematical calculation [43].

Item	C_P (J/kg K)	Absorptivity	Emissivity
Non-potable water	4190	0.050	0.960
Glazier cover	840	0.050	0.850
Basin plate	460	0.950	–

h_{fg} = 2,335,000 J/kg.

2.4. System performance estimation

To estimate the practicability of current system in a correct manner, many parameters are used.

The thermal performance for HDH is expressed by GOR as [10]

$$GOR_{HDH} = \frac{m_{dHDH} h_{fg}}{Q_{in\ total}} \quad (23)$$

A high GOR is preferable since it indicates that less heat input is demanded per unit fresh water.

The overall thermal performance of the hybrid desalination unit is computed as [15]

$$GOR_{sys} = GOR_{HDH} + GOR_{FSS} \quad (24)$$

The daily efficiency for solar still, η_d is calculated by Eq. (19).

The value of $Q_{intotal}$ = [Q_{solar} + (power of pumps and fan)] used to carry out the calculations that lead to the claimed GOR was about 7000 W. Also, during the breakup of HDH system from 8 am to 13 pm, the solar radiation enters the evacuated tub solar collectors to heat water before HDH operation from 13 to 18 then the overall $Q_{intotal}$ was used during the whole day time.

3. Results and discussion

3.1. Humidification-Dehumidification productivity

The experimental results pointed out that maximum solar intensity was about 1100 W/m^2. The water temperature was about 87 °C in the collector due to stored energy inside the collector. Fig. 2 shows the variation of the solar radiation and the cumulative productivity with time during three different days. From the figure, the first hour (13:00–14:00 pm) of operation gave the extreme yield of nearly 13.5 kg due to the higher temperature of water entering the humidifier from solar collector, then the yield reduced till it reaches the minimum value of about 1 kg at (17:00–18:00 pm) owing to the lower temperature of the water entered the humidifier. The cumulative productivity reached a value of approximately 24 kg per day. The experimental system was started up at 13:00 pm and was left for a long period to reach steady sate conditions to take the measurements. The operating parameters were as follows: airflow rate were about 0.018 kg/s and the flow of hot and cold water were 0.0416 kg/s.

Humidity (moisture) ratio is used as a simple tool to express humidification and dehumidification in HDH unit. The variation of humidity ratio with time is shown in Fig. 3. The moisture ratio at humidifier (evaporator) exit equals to the moisture ratio at dehumidifier (condenser) inlet. The humidity ratio at dehumidifier exit equals to the humidity ratio at humidifier inlet. The results indicated that at humidifier outlet, the moisture ratio almost gave higher values than that of the dehumidifier outlet all the time. Moreover, the variation of moisture ratio at the first time operation was much larger due to the high water temperature.

The amount of rejected warm water from HDH was calculated by the following equations $m_{w\ reje} = m_w \times t$, where $m_{w\ reje}$ is the amount of rejected warm water from HDH, m_w is the hot water flow rate and t is the time of operation for the first 5 h of the HDH operation period, i.e., from 13 to 18 pm,

$$m_{w\ reje} = 2.4 \times 5 \times 60 = 720\ \text{kg}.$$

However, currently the rejected warm water was used only at the first three hours of the HDH operation period due to increase of the water temperature significantly. Hence, the actual water amount which was used to feed FSS can be calculated as follows

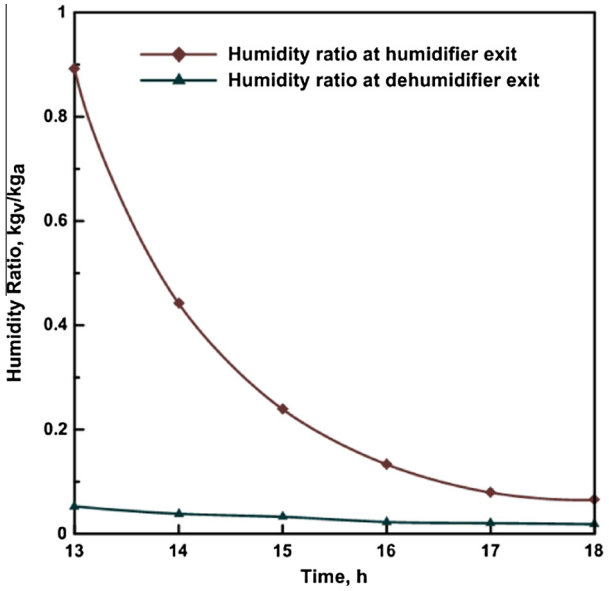

Fig. 3. Humidity ratio versus time at humidifier outlet and dehumidifier outlet.

$m_{w\ reje,FSS} = 2.4 \times 3 \times 5 = 432$ kg.

This amount of rejected warm water was enough to operate the FSS units.

3.2. Effect of the insulation thickness

Fig. 4 illustrates the performance of the SS with insulation (glass-wool with thermal conductivity of 0.047 kW/m K) with a thickness ranged from 0.03 to 0.1 m. From the figure, increasing the insulation thickness affects positively both the productivity and the efficiency of the SS till it reaches a value of 0.03 m paid to increasing the working temperature. Moreover, during the day time, the peripheral temperature increased with the increase of insolation. So, the losses will be decreased. Hence, the required insulation thickness was about 0.02 m. On the other hand, during night time, the best insulation thickness was found to be 0.03 m, because the demise of the solar radiation and the low temperature of the peripheral which increase the losses. To overcome this high loss, the insulation thickness must be increased.

The insulation thickness beyond 0.03 m has a slight effect on the performance. The use of perfect insulation and hot water improves the efficiency and the yield to reach 10 kg/day and 90%, respectively (during day and night). There is an agreement between the former result and Khalifa and Hamood [16]. They found that complete insulation of SS enhances the productivity by 80%. The improvement in the daily productivity resulted from increasing the insulation thickness, which decreased the heat loss and then increased the productivity. Moreover, feeding hot water from insulated storage tank gave a significant increase in the productivity.

3.3. Effect of insolation on the solar still performance

The change of solar intensity, base plate temperature, basin non-potable water and glass (glazier) cover temperature of SS are shown in Fig. 5. It was noticed that the temperature at all points increased with the time until the noon when the maximum value was reached.

3.4. Solar still fresh water yield

The theoretical variations of the freshwater yield per hour of the studied SS are illustrated in Fig. 6. Makeup occurs every hour. From the figure, it was detected that the freshwater yield increased in the early (morning) hours of the day till it reached the peak at mid-noon because of the highest solar intensity, then reduces at the time of sun set. Additionally, it was found that maximum temperature of non-potable water gave the extreme yield. Fig. 6 shows that the water productivity was about 0.45 and 1.8 kg/h for SSs and FSS, respectively in the morning hours (due to the use of hot water from the insulated tank and no need to warm up) and reached up to an extreme yield of approximately 1.18 and 4.7 kg/h for SSS and FSS, respectively, at 13 p.m. Hence, at the mid-noon, the thermal losses of the SS were low and the performance enhanced proportionally. Also, from Fig. 6, the water production in CSS increased from the lowest (zero) value in the morning and reached its maximum value in the afternoon. This is due to the relatively low tem-

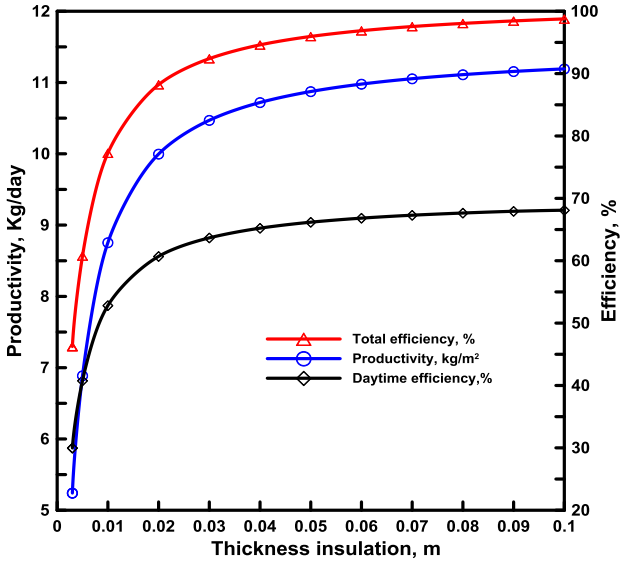

Fig. 4. Efficiency and productivity with thickness of insulation.

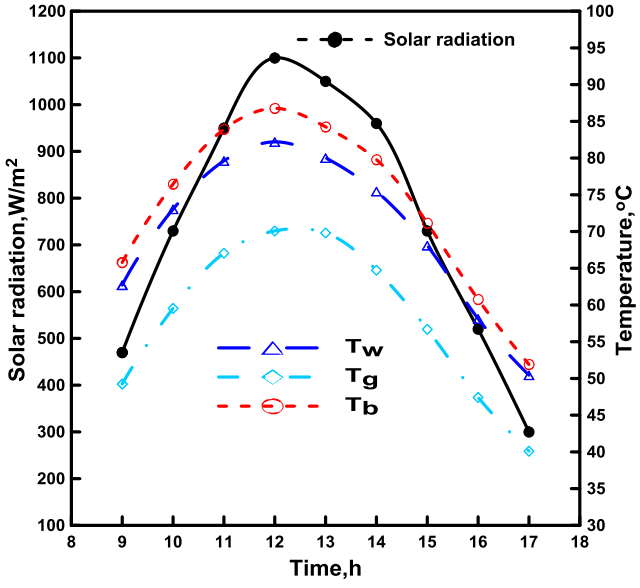

Fig. 5. Hourly temperature changes and solar intensity for SS.

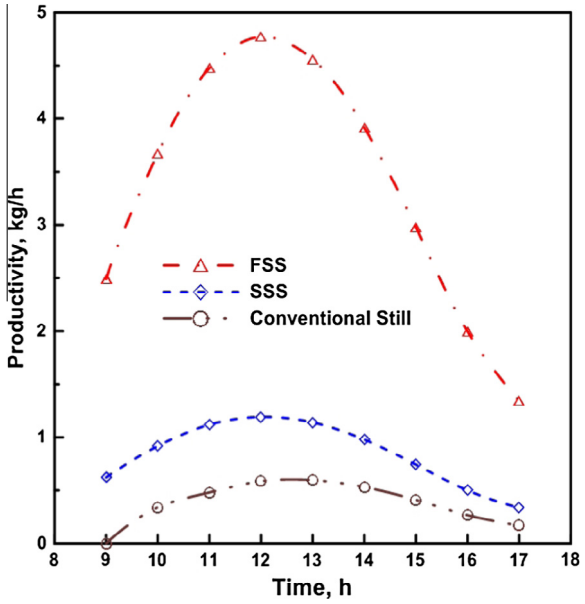

Fig. 6. Freshwater Productivity Through Daytime.

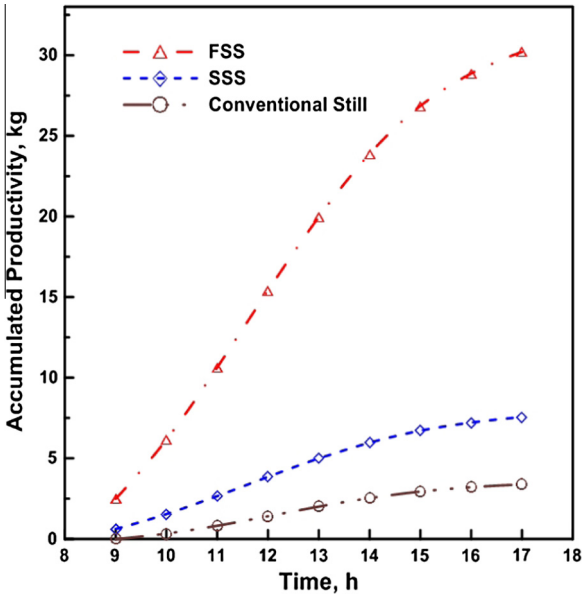

Fig. 7. Accumulative productivity through the daytime.

perature of water in the SS in the early time of the day and water needs extra time to be heated. Fig. 7 shows the accumulative productivity of the freshwater per hour from 9:00 am to 17:00 pm. The daily yield (productivity) for both CSS, SSS and FSS reaches approximately 3.2, 7.5 and 30 kg/day, respectively.

3.5. Effect of feeding hot non-potable water through nighttime on the solar still output

Isolated storage tank was used to feed water to the FSS during night times (replace all water in the basin every hour by hot water from isolated tank). Fig. 8 illustrates the prediction of freshwater yield per hour during night times (from 17:00 pm to 8:00 am of the second day) at inlet water temperatures of about 65 °C. The ambient temperature was in the range of 21.5–26 °C, whereas wind speed was in the range of 1.3–2.5 m/s through the mean

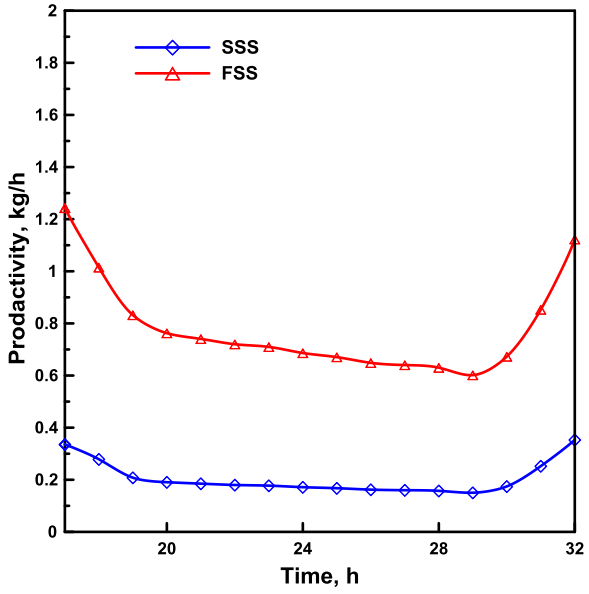

Fig. 8. Hourly variation of productivity for SSs and FSS through nighttime.

measurement day. During the wee hours of the night, productivity decreases gradually because of the decrease of environmental air temperature, the increase of the temperature variation between the still and the surrounding and the increase of heat losses. While, the early hours of the second day cause an increase in the yield due to sunrise, decrease the temperature variation between the still and surrounding and the decrease of heat losses. Fig. 9 presents the cumulative productivity through night times that reaches a value of about 3 and 12 kg for SSS and FSS, respectively.

3.6. Hybrid system productivity

Fig. 10 shows the accumulative fresh water production of the unit during day and night times. The accumulative freshwater production improved with intensification the solar radiation intensity and vice versa. The daily water production of the SSS, FSS, HDH and hybrid (HDH-FSS) system were 10.5, 42, 24.3, and 66.3 kg/day, respectively.

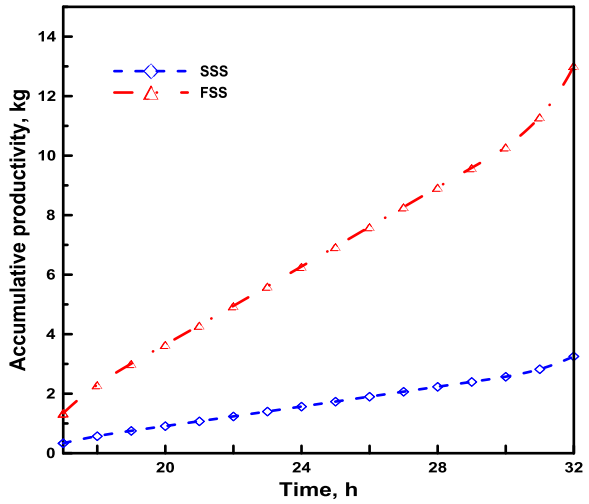

Fig. 9. Accumulative productivity through the nighttime.

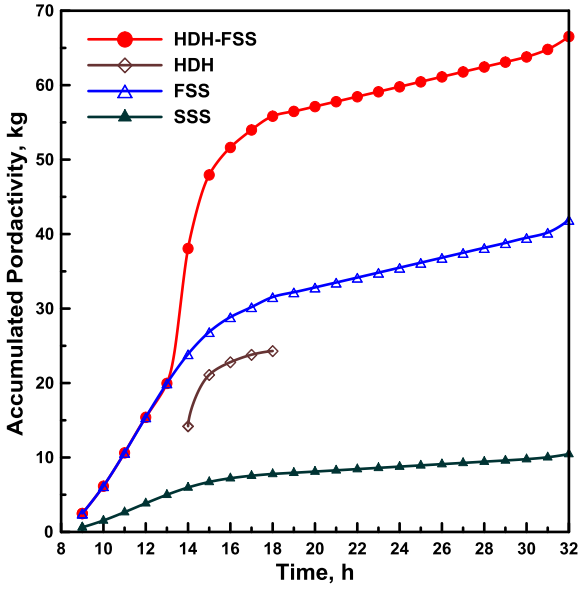

Fig. 10. Cumulative freshwater productivity through day and night time for SSS, FSS, HDH and HDH-FSS.

4. System performance

The system performance is discussed in this section. HSDS (HDH–FSS) cycles are classically heat driven cycles working by low-grade energy to heat the non-potable water. The efficiency of the cycle itself was measured by the GOR as defined in Eqs. (23) and (24). The average GOR of the HDH unit was about 2.14. While, the GOR trend of FSS units was constant and nearly equal unity. Therefore, GOR of the HSDS system reached 3.18. GOR increased by 50% due to using the FSS during nighttime.

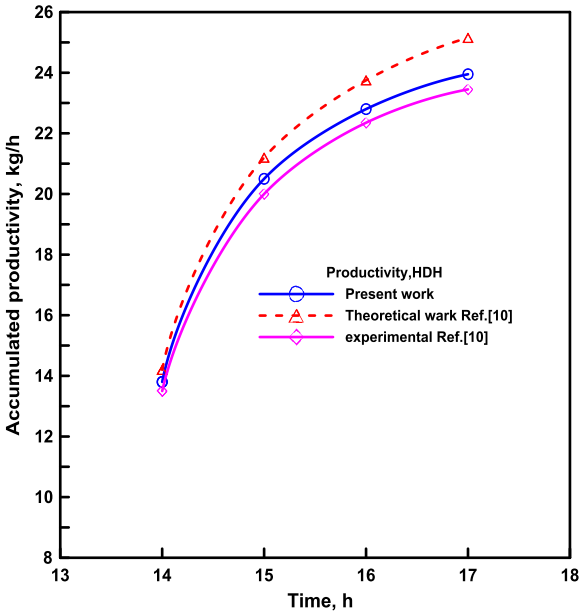

Fig. 11. Comparing the cumulative productivity, HDH between the present work and Ref. [10].

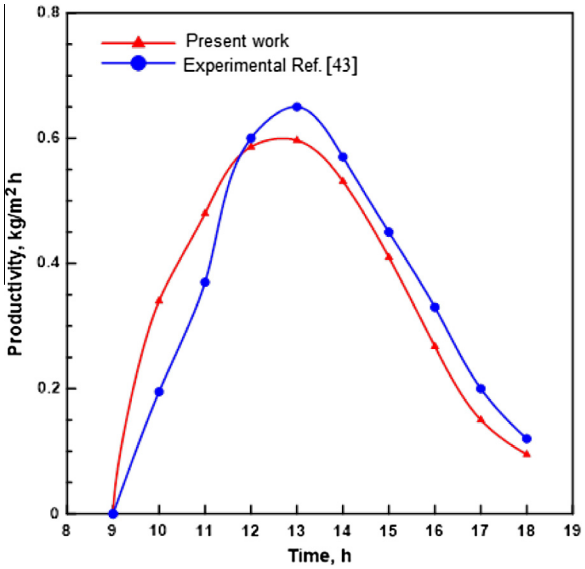

Fig. 12. Comparing between the present work CSS and Omara et al. [43] of hourly productivity for CSS.

5. Present work validation

Hamed et al. [10] studied mathematically and experimentally the evaluation performance of HDH. Fig. 11 presents a comparison between the present work of HDH and [10] at the same conditions. The output results for cumulative productivity of HDH show a good agreement between the two works. While, Fig. 12 shows an agreement to a great extent between the present theoretical work for CSS and the experimental work by Omara et al. [43] at the same conditions. The comparison between present study and previous work about HDH and CSS is presented in Table 4.

6. Cost evaluation

The price of the solar distillation unit is a significant factor. Cost of the SS relies mainly on productivity which, in turn the latter relies on the intensity of the solar radiation. The solar radiation intensity changes due to the location of the SS. In this point, the selection of the place has a large impact on the cost.

6.1. Cost estimation for humidification-dehumidification

The overall fixed price of HDH is nearly F = 1442$ as shown in Table 5 as stated in [10]. Important parameters should be introduced for obtaining the average value of the cost, such as: N is the expected life time of HDH, V is the changeable cost and C is the overall price where C = F + C. Consider changeable price (maintenance) V equals to 20% of fixed price per year as stated in [10] and the expected HDH life is 10 years, then C = 1442

Table 4
Comparing between different research works and present study about HDH or CSS systems.

References	Max. productivity (kg/day)	Price per liters ($)
Present study (hybrid system)	63.3	0.034
Nafey et al. [8,9], HDH	10.25	Not given
Hamed et al. [10], HDH	22	0.058
Omara et al. [27], CSS	3.5	0.049
Omara et al. [43], CSS	3.72	0.049

Table 5
Price of fabricated of unit system.

Unit	Price of HDH US$ [10]	Price of FSS [20] US$	Price of HSDS, US$
Unit price	500	33 × 4 = 132	632
Coil of heat exchanger	180	–	180
Packing materials	70	–	70
Ducts	15	3 × 4 = 12	27
Paint and silicon	15	12 × 4 = 48	63
Insulation	50	5 × 4 = 20	70
Production	150	25 × 4 = 100	250
Support legs	12	11.5 × 4 = 46	58
Fan and pumps	150	75	225
Glazier cover	–	6 × 4 = 24	24
Solar collector	300	–	300
Overall fixed price (F)	1442	457	1899

+ 0.2 × 1442 × 10 = 4326$. The minimum average daily yield can be calculated from the analysis of various experimental data to be 22 kg/day. Considering that HDH carries out 340 days per year as the sun rises throughout the year in Egypt so, the overall productivity during the HDH life is P_n = 74,800 kg. As a result, the overall price for one liter produced from HDH = 4326/74800 = 0.0578$.

6.2. Cost estimation for conventional still

The overall fixed cost of CSS is nearly F = 103$ as stated in Table 5 as in [20]. For obtaining the average value of the distillate output cost, it is important to consider that V is the changeable cost and C is the overall cost, where C = F + V. Consider changeable cost V equals 0.3F per year, as stated in [44], then C = 103 + 0.3 × 103 × 10 = 412$. The minimum average daily yield can be determined from the analysis of various experimental data and it is taken as 2.5 kg/day stated in [20]. To calculate the annual cost for one liter, considering that the still runs out 340 days throughout the year where the sun rises throughout the year in Egypt. The predicted still life time is 10 years. The overall yield during the still life time = 2.5 × 10 × 340 = 8500 kg. The cost of one liter produced from CSS = 412/8500 = 0.049$.

6.3. Cost estimation for hybrid system

The overall fixed price of hybrid system is nearly F = 1899$. Consider the predicted life of the hybrid system is 10 years. Consider changeable price (maintenance) V equals to 30% of fixed price per year so V = 0.3*F*, then C = 1899 + 0.3 × 1899 × 10 = 7596$ where the minimum average daily productivity can be taken as 45.5 kg/day considering unit carries out 340 days throughout the year. The overall yield during the unit life is Pn = 154,700 kg. From the former analysis, it can be found that the price of one liter produced from hybrid is nearly (7596/154,700) = 0.034$.

7. Conclusions

A hybrid solar desalination system (HSDS) reuses the drain warm water from humidification-dehumidification unit to feed solar stills to prevent massive water loss during HDH desalination. Reusing the drain water increases the GOR of the system by 50% and increases the efficiency of single SS to about 90%. Furthermore, the productivity of a single solar still, as a part of the hybrid system, is more than that of a CSS approximately by 200%. The daily water production of the CSS, SSS, FSS, HDH and HSDS are 3.2, 10.5, 42, 24.3 and 66.3 kg/day, respectively. Furthermore, the cost per unit liter of distillate from CSS, HDH and HSDS are around $0.49, $0.058 and $0.034, respectively.

Acknowledgements

N.Y. was sponsored by the National Natural Science Foundation of China – China (No. 51576076). The authors express their sincere appreciation to College of Engineering at Kafrelsheikh University for moral support and financial funding during experimentation.

Appendix A

$$Gr' = \frac{\beta_1 \times g \times d^3 \times \rho^2 \times \Delta T'}{\mu^2}$$

$$\Delta T' = \frac{(T_w - T_g) + (P_w - P_g) + (T_w + 273)}{(268.9 \times 10^3 - P_g)}$$

$$Pr = \frac{\mu \times C_p}{k}$$

$$C_p = 999.2 + 0.1434 \times T_i + 1.0101 \times 10^{-4} \times T_i^2 - 6.7581 \times 10^{-8} \times T_i^3$$

$$\rho = \frac{353.44}{(T_i + 273.15)}$$

$$T_i = \frac{(T_w + T_g)}{2}$$

$$k = 0.0244 + 0.7673 \times 10^{-4} \times T_i$$

$$\mu = 1.718 \times 10^{-5} + 4.62 \times 10^{-8} \times T_i$$

$$\beta_1 = \frac{1}{(T_i + 273)}$$

$$(70 \prec T_i): \; h_{fg} = 3.1615 \times \left[10^6 - 761.6 \times T_i\right]$$

$$(T_i \prec 70): \; h_{fg} = 2.4953 \times \left[10^6 - 947.79 \times T_i + 0.13132 \times T_i^2 - 0.0047974 \times T_i^3\right]$$

References

[1] Shannon MA, Bohn PW, Elimelech M, Georgiadis JG, Marinas BJ, Mayes AM. Science and technology for water purification in the coming decades. Nature 2008;452:301–10.
[2] Frisbie SH, Mitchell EJ, Dustin H, Maynard DM, Sarkar B. World health organization discontinues its drinking-water guideline for manganese. Environ Health Perspect 2012;120:775–8.
[3] Karuppusamy S. An experimental study on single basin solar still augmented with evacuated tubes. Therm Sci 2012;16:573–81.
[4] Zhou L, Tan Y, Wang J, Xu W, Yuan Y, Cai W, et al. 3D self-assembly of aluminium nanoparticles for plasmon-enhanced solar desalination. Nat Photon 2016 [Advance online publication].

[5] Narayan GP, Sharqawy MH, Summers EK, Lienhard JH, Zubair SM, Antar MA. The potential of solar-driven humidification–dehumidification desalination for small-scale decentralized water production. Renew Sustain Energy Rev 2010;14:1187–201.
[6] Kabeel AE, Hamed M, Omara Z, Sharshir S. Water desalination using a humidification–dehumidification technique—a detailed review. Nat Resour 2013;4:286–305.
[7] Mohamed AMI, El-Minshawy NA. Theoretical investigation of solar humidification–dehumidification desalination system using parabolic trough concentrators. Energy Convers Manage 2011;52:3112–9.
[8] Nafey AS, Fath HES, El-Helaby SO, Soliman AM. Solar desalination using humidification dehumidification processes. Part I. A numerical investigation. Energy Convers Manage 2004;45:1243–61.
[9] Nafey AS, Fath HES, El-Helaby SO, Soliman A. Solar desalination using humidification–dehumidification processes. Part II. An experimental investigation. Energy Convers Manage 2004;45:1263–77.
[10] Hamed MH, Kabeel AE, Omara ZM, Sharshir SW. Mathematical and experimental investigation of a solar humidification–dehumidification desalination unit. Desalination 2015;358:9–17.
[11] Ghazal MT, Atikol U, Egelioglu F. An experimental study of a solar humidifier for HDD systems. Energy Convers Manage 2014;82:250–8.
[12] Malli A, Seyf HR, Layeghi M, Sharifian S, Behravesh H. Investigating the performance of cellulosic evaporative cooling pads. Energy Convers Manage 2011;52:2598–603.
[13] Nafey AS, Mohamad MA, El-Helaby SO, Sharaf MA. Theoretical and experimental study of a small unit for solar desalination using flashing process. Energy Convers Manage 2007;48:528–38.
[14] Yıldırım C, Solmuş İ. A parametric study on a humidification–dehumidification (HDH) desalination unit powered by solar air and water heaters. Energy Convers Manage 2014;86:568–75.
[15] Hou S, Zhang H. A hybrid solar desalination process of the multi-effect humidification dehumidification and basin-type unit. Desalination 2008;220:552–7.
[16] Khalifa AJN, Hamood AM. Effect of insulation thickness on the productivity of basin type solar stills: an experimental verification under local climate. Energy Convers Manage 2009;50:2457–61.
[17] Tchinda R, Kaptouom E, Njomo D. Heat and mass transfer processes in a solar still with an indirect evaporator–condenser. Energy Convers Manage 2000;41:93–107.
[18] Khalifa AJN, Hamood AM. On the verification of the effect of water depth on the performance of basin type solar stills. Sol Energy 2009;83:1312–21.
[19] Abu-Hijleh BAK, Rababa'h HM. Experimental study of a solar still with sponge cubes in basin. Energy Convers Manage 2003;44:1411–8.
[20] Omara ZM, Kabeel AE, Younes MM. Enhancing the stepped solar still performance using internal and external reflectors. Energy Convers Manage 2014;78:876–81.
[21] Kabeel AE, Abdelgaied M. Improving the performance of solar still by using PCM as a thermal storage medium under Egyptian conditions. Desalination 2016;383:22–8.
[22] El-Sebaii AA. Effect of wind speed on active and passive solar stills. Energy Convers Manage 2004;45:1187–204.
[23] Al-Hinai H, Al-Nassri MS, Jubran BA. Effect of climatic, design and operational parameters on the yield of a simple solar still. Energy Convers Manage 2002;43:1639–50.
[24] Sharshir SW, Yang N, Peng G, Kabeel AE. Factors affecting solar stills productivity and improvement techniques: a detailed review. Appl Therm Eng 2016;100:267–84.
[25] Experimental studies on a solar still coupled with a flat-plate collector and a single basin still. Energy Convers Manage 1998;39:853–6.
[26] Yadav YP. Analytical performance of a solar still integrated with a flat plate solar collector: thermosiphon mode. Energy Convers Manage 1991;31:255–63.
[27] Omara ZM, Eltawil MA, ElNashar EA. A new hybrid desalination system using wicks/solar still and evacuated solar water heater. Desalination 2013;325:56–64.
[28] Velmurugan V, Gopalakrishnan M, Raghu R, Srithar K. Single basin solar still with fin for enhancing productivity. Energy Convers Manage 2008;49:2602–8.
[29] El-Agouz SA, El-Samadony YAF, Kabeel AE. Performance evaluation of a continuous flow inclined solar still desalination system. Energy Convers Manage 2015;101:606–15.
[30] Samuel DG Harris, Nagarajan PK, Sathyamurthy R, El-Agouz SA, Kannan E. Improving the yield of fresh water in conventional solar still using low cost energy storage material. Energy Convers Manage 2016;112:125–34.
[31] Kabeel AE, Abdelgaied M, Mahgoub M. The performance of a modified solar still using hot air injection and PCM. Desalination 2016;379:102–7.
[32] Omara ZM, Kabeel AE, Essa FA. Effect of using nanofluids and providing vacuum on the yield of corrugated wick solar still. Energy Convers Manage 2015;103:965–72.
[33] Kabeel AE, Hamed MH, Omara ZM, Sharshir SW. Experimental study of a humidification–dehumidification solar technique by natural and forced air circulation. Energy 2014;68:218–28.
[34] Velmurugan V, Pandiarajan S, Guruparan P, Subramanian LH, Prabaharan CD, Srithar K. Integrated performance of stepped and single basin solar stills with mini solar pond. Desalination 2009;249:902–9.
[35] Murugavel K Kalidasa, Sivakumar S, Ahamed J Riaz, Chockalingam KKSK, Srithar K. Single basin double slope solar still with minimum basin depth and energy storing materials. Appl Energy 2010;87:514–23.
[36] Velmurugan V, Kumaran SS, Prabhu NV, Srithar K. Productivity enhancement of stepped solar still: performance analysis. Therm Sci 2008;12:153–63.
[37] Velmurugan V, Kumar KJ Naveen, Haq T Noorul, Srithar K. Performance analysis in stepped solar still for effluent desalination. Energy 2009;34:1179–86.
[38] Zoori H Aghaei, Tabrizi F Farshchi, Sarhaddi F, Heshmatnezhad F. Comparison between energy and exergy efficiencies in a weir type cascade solar still. Desalination 2013;325:113–21.
[39] Dev R, Tiwari GN. Characteristic equation of a passive solar still. Desalination 2009;245:246–65.
[40] Zurigat YH, Abu-Arabi MK. Modelling and performance analysis of a regenerative solar desalination unit. Appl Therm Eng 2004;24:1061–72.
[41] Velmurugan V, Deenadayalan CK, Vinod H, Srithar K. Desalination of effluent using fin type solar still. Energy 2008;33:1719–27.
[42] Murugavel K Kalidasa, Srithar K. Performance study on basin type double slope solar still with different wick materials and minimum mass of water. Renew Energy 2011;36:612–20.
[43] Omara ZM, Kabeel AE, Younes MM. Enhancing the stepped solar still performance using internal reflectors. Desalination 2013;314:67–72.
[44] Mukherjee K, Tiwari GN. Economic analyses of various designs of conventional solar stills. Energy Convers Manage 1986;26:155–7.